Jurnal Teknologi, 30(D): 33–54

THE LAG WINDOWED WIGNER-VILLE DISTRIBUTION: AN ANALYSIS METHOD FOR HF DATA COMMUNICATION SIGNALS

AHMAD ZURI SHA'AMERI[1] & BOUALEM BOASHASH[2]

Abstract. The focus of the paper is on the estimation of modulation parameters for digital modulation signals such as FSK (Frequency Shift-Keying) and ASK (Amplitude Shift-Keying) used in HF (High Frequency) radio communications. Time-frequency signal analysis techniques are proposed and the new time-frequency distribution developed is known as the lag-windowed Wigner-Ville distribution. The modulation parameters of the signals such as the subcarrier frequencies, and the bit-rate can be extracted directly from the time-frequency representations. The LWWVD improves the time-frequency representation by minimizing the interference terms due to the cross-terms. Comparisons with the conventional Wigner-Ville distribution (WVD), reduced interference distributions (RID) and other related methods are made based on the criteria of the mainlobe width and the peak-to-sidelobe ratio. Consistently, the LWWVD gives the most accurate time-frequency representation for ASK and FSK signals at high signal-to-noise ratio conditions.

1.0 INTRODUCTION

Radio monitoring systems are used in spectrum management to verify conformance to the frequency allocations and as tools in the detection, estimation and classification of radio transmissions. The ITU-R (International Telecommunication Union-Radio) in [1] outlined the framework for managing the radio frequency spectrum and the general features of a radio monitoring system are described in Figure 1. The study is focused on the modulation parameter estimation for digital modulation signals and the chosen method is based on time-frequency signal analysis. Examples of the modulation parameters of the signals are the subcarrier frequencies, deviation frequency, bit-rate and the phase-shift. By estimating the modulation parameter, a received signal can be classified and a receiver can be set to recover the binary information from the signal. The digital modulation signals considered in this paper are the ASK and FSK signals for the HF (High Frequency) radio frequency spectrum. The signals were chosen because these are the most common digital modulation methods used in the HF data communication

[1] Faculty of Electrical Engineering, Universiti Teknologi Malaysia, 81310 UTM Skudai, Johor Bahru, Malaysia. e-mail: ahmadzs@safenet.utm.my

[2] Signal Processing Research Centre, Queensland Univ of Technology, P.O. Box 2434, Brisbance 4001, Australia. e-mail: b.boashash@qut.edu.au

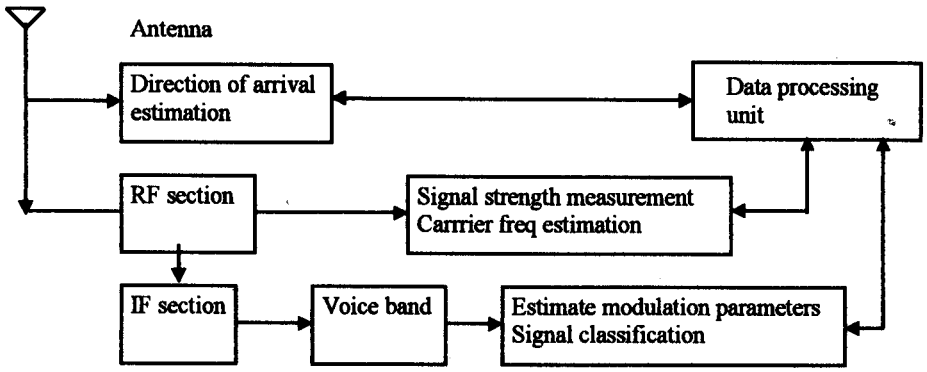

Figure 1 Block diagram of a radio manitoring system. [The data processing unit controls all the measurement functions, performs data logging and provides the interface to the operator. The focus of this paper is on the estimation of modulation parameters for digital modulation signals.]

systems [2]. However, the research findings can be applied to other data signals used in the VHF (Very High Frequency) and UHF (Ultra High Frequency) range.

Two general methods that are used for estimation and classification of digital modulation signals are the likelihood or decision-theoretic method [3]-[4] and the pattern recognition method [5]-[6]. The decision-theoretic method uses the likelihood function conditioned to a known set of candidate signals to classify an unknown signal. The decision-theoretic method are used for PSK [4] and FSK [5]. In the pattern recognition method, the estimated modulation parameters are used as the extracted features of the signal and are matched to its corresponding type by classifier network. Application examples of the pattern recognition approach are demonstrated in [11]-[14] for ASK, FSK and PSK. Some methods that have been used to estimate the modulation parameters include frequency and phase histograms [5], zero-crossings [6], cyclic spectrum [7] and AR (autoregressive) modelling [8]. A limitation of the decision-theoretic approach is that it requires the exact form of the candidate set of signals to generate the likelihood function. However, this may not occur in practice since the exact form of the received signal is not known. Thus, the pattern recognition approach is more practical method to use since only the features of the signal are used in the classifier.

The Wigner-Ville distribution was developed as a method to analyze nonstationary signals [9]. The general formulation for bilinear time-frequency distribution was described in [10] and the various time-frequency distributions

such as the Wigner-Ville distribution, reduced interference distributions [11], and the spectrogram are determined by the choice of the kernel functions. Recent developments in time-frequency signal analysis are in higher-order time-frequency representation [12], adaptive spectrogram [13], and windowed Wigner-Ville distribution [14]. Time-frequency signal analysis was also used in the in spread spectrum communications [15]. The research extends the work of [16]-[17] on the analysis of digital modulation signals based on the windowed Wigner-Ville distribution. A time-dependent window is introduced in the windowed Wigner-Ville distribution and the result is a more accurate time-frequency representation. The proposed time-frequency distribution is known as the lag-windowed Wigner-Ville distribution. From the time-frequency representations, the modulation parameters of the signal can be estimated and the binary information contained in the signal information can be recovered. This is an advantage compared to other signal analysis methods [2]-[8] where a separate algorithm is required to recover the binary information. The paper is organized as follows: Section 2 defines the signal models and the assumptions, Section 3 introduces the Wigner-Ville and the windowed Wigner-Ville distribution and the interference problems in the time-frequency representations, Section 4 will propose solutions to the problem using the lag-windowed Wigner-Ville distribution, and Section 5 will present the results and compare with existing techniques.

2.0 MODEL FOR DIGITAL MODULATED SIGNALS

A generalized model for a time-varying signal is given by [18]

$$z(t) = c(t)\exp(j2\pi \int_{-\infty}^{t} f_i(\lambda)d\lambda + \phi(t)) + n(t) \qquad (1)$$

where $c(t)$ is the time-varying amplitude of the signal, $f_i(t)$ is the instantaneous frequency, $\phi(t)$ is the time-varying phase of the signal and $n(t)$ represents the interference due to noise. If applied to digital modulated signals, the possible classes of signals obtained from Equation (1) are:

1 ASK (Amplitude Shift-Keying) – $c(t)$ varies, $f_i(t)$ and $\phi(t)$ are constant.
2 FSK (Frequency Shift-Keying) – $f_i(t)$ varies, $\phi(t)$ and $c(t)$ are constant.
3 PSK (Phase Shift-Keying) – $\phi(t)$ varies, $f_i(t)$ and $c(t)$ are constant.

The digital modulation signals used for analysis are HF data communications signals where the binary data are modulated at the voiceband frequencies using subcarriers. Another common method for transmitting information is by telegraphy using Morse code. Since information is represented as a series of

dots and dashes, telegraphy signals can be considered similar to ASK signals where the dots are represented zero amplitude and dashes as sinusoids. Further details on digital communication requirements can be found in the ITU-R recommendations and reports [2]. Examples of simulated ASK and FSK signals used for analysis are presented in Table 1.

Table 1 The various digital modulated signals defined within the bit-duration T_b of 10 msec. [$c(t)$ is the filter impulse response]

Signal Name	Binary data s(t)	$z(t)$ where $t_0 < t < t_0 + T_b$	Binary Sequence
FSK0	1	$c(t)exp(j(2\pi 1400t))$	101010
	0	$c(t)exp(j(2\pi 1800t))$	
FSK1	1	$c(t)exp(j(2\pi 1000t))$	101010
	0	$c(t)exp(j(2\pi 1400t))$	
FSK0a	1	$c(t)exp(j(2\pi 1400t))$	1110100
	0	$c(t)exp(j(2\pi 1800t))$	
ASK0	1	$c(t)exp(j(2\pi 1000t))$	101010
	0	0	
ASK0a	1	$c(t)exp(j(2\pi 1000t))$	1110100
	0	0	

Signals FSK0 and FSK0a are considered to be of the same type because the modulation parameters are the same. Only the binary sequence transmitted determines the difference between the two signals. Similarly this is also true for the signals ASK0 and ASK0a. The two examples are chosen because in practice the exact sequence transmitted is unknown and random in nature. The simulated signals are chosen to assess whether the existing and proposed time-frequency analysis methods can produce accurate time-frequency representations regardless of the signal class, signal type and the binary information content of the signal.

In HF data communication, the duration of transmission depends on the length of the information. For analysis purposes, it is not necessary to analyze the signal for the duration of transmission since a sample of the whole process is enough to estimate the modulation parameters of the signal. An analysis frame of 64 msec is used to analyze of the signal and the duration is sufficient to include at least 5 bits of the transmitted binary sequence. The choice on the analysis frame is constrained by the accuracy and the computation time. Since the typical bandwidth of an HF channel is 4000 Hz, a sampling frequency of 8000 Hz can be used based on the Nyquist sampling rate. At 64 msecs of analysis frame, the number of samples is 512 with a spectrum resolution of 15.6 Hz/frequency sample.

The time domain representation and spectrum for the simulated signal FSK0 is shown in Figure 2. Examples of time domain representations and spectrums for real HF data communication signals are shown in Figure 3 and 4. The signal in Figure 3 is an FSK signal that is referred as signal FSK2 while the ASK signal in Figure 4 is referred as signal ASK2.

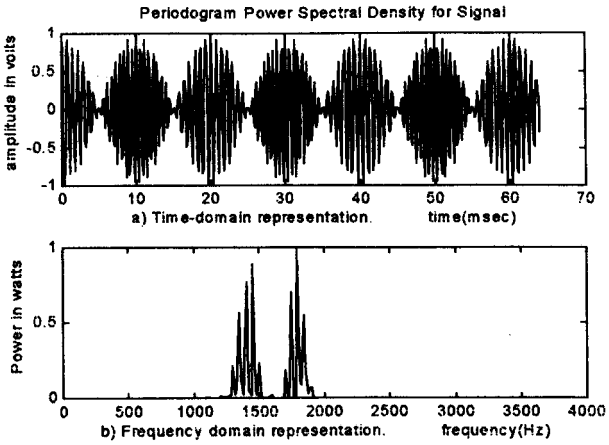

Figure 2 Time and frequency representations for signal FSKO. [A periodic '101010' sequence is assumed in this signal. At $15 < t < 25$ msec, the frequency is 1400 Hz, and at $25 < t < 35$ msec, the frequency is 1800 Hz.]

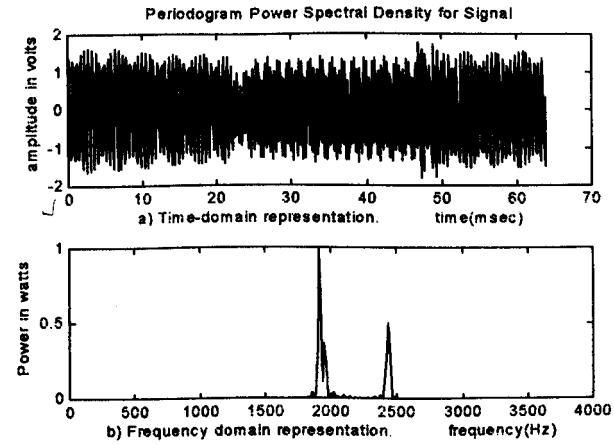

Figure 3 Time and frequency representations for real FSK signal (signal FSK2). [The subcarrier frequencies of the signal is 1.9 and 2,4 KHz, and the bit-rate is 40 bits/sec.]

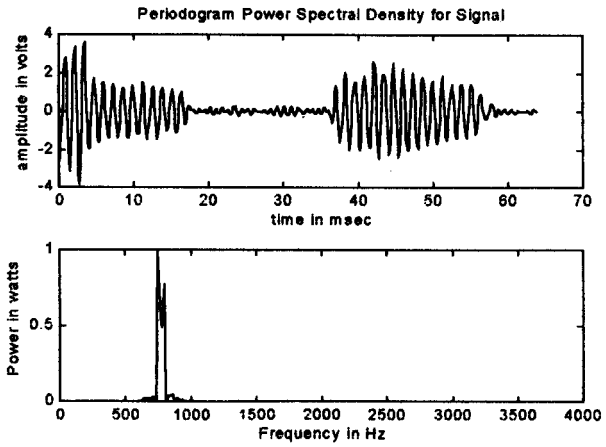

Figure 4 Time and frequency representations for real ASK signal (signal ASK2). [The subcarrier frequency is 700 Hz and the bit-rate is 50 bits/sec.]

3.0 TIME-FREQUENCY DISTRIBUTION

The generalized formulation for bilinear time-frequency distributions is defined as [10]

$$\rho_z(t,f) = \int_{-\infty}^{\infty}\int_{-\infty}^{\infty} g(u,\tau)z(t-u+\tau/2)z^*(t-u-\tau/2)\exp(-j2\pi f\tau)\,du\,d\tau \quad (2)$$

where $g(u,\tau)$ is the time-lag kernel function and $z(t)$ is the signal in analytical form. In the above equation, the product $z(t+\tau/2)z^*(t-\tau/2)$ will be referred as the bilinear product. The various time-frequency distributions such as the Wigner-Ville distribution and the class of reduced interference distributions may be obtained based on the choice of the kernel functions.

By assuming the kernel function as a delta function in time, the Wigner-Ville distribution (WVD) can be derived from Equation (2) and is defined as

$$W_z(t,f) = \int_{-\infty}^{\infty} z(t+\tau/2)z^*(t+\tau/2)\exp(-j2\pi f\tau)\,d\tau \quad (3)$$

The distribution meets most of the desired properties for time-frequency distributions [10].

A window function is used to localize the Wigner-Ville distribution and minimize interference in the time-frequency representation. The windowed Wigner-Ville distribution (WWVD) [10] is

$$W_{z,w}(t,f) = \int_{-\infty}^{\infty} h(\tau)z(t+\tau/2)z^*(t-\tau/2)\exp(-j2\pi f\tau)d\tau \qquad (4)$$

where $h(\tau)$ is the window function. The positive real window function is such that $h(\tau) > 0$ for the interval $-\tau_{win}/2 < \tau < \tau_{win}/2$. The choice of the length and type of the window function can be chosen to minimize interference for a given class of signal.

From the time representation of FSK0 in Figure 2, only one frequency component must be present at any given time instant. However, this is not reflected in the WVD in Figure 5 where more than one frequency is present at a given time instant on the time-frequency representation. A relatively more accurate time-frequency representation as shown in Figure 7 using the WWVD.

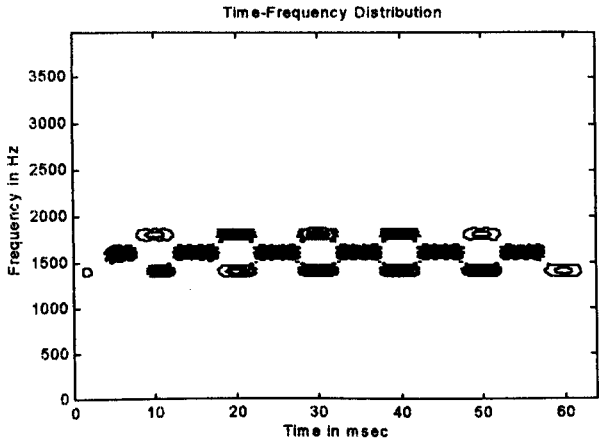

Figure 5 Wigner-Ville distribution for signal FSKO. [At $15 < t < 25$ msec and $25 < t < 35$ msec, more than one frequency component appeared on the time-frequency representation.]

The interference in the time-frequency representations can be explained by observing the variation in the bilinear product in Figure 6. The interference components is present in the WVD because the Fourier transform performed on the bilinear product over lag includes both desired and interference components. By having a window function, the WWVD only considers the desired signal components in the bilinear product. Thus, the Fourier transform over lag will represent only the desired frequency component.

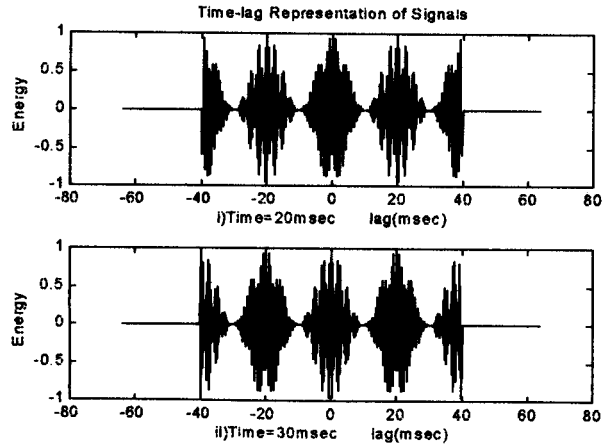

Figure 6 Bilinear product for signal FSKO evaluated at time $t = 20$ and 30 msec. [The bilinear product varies in frequency over the lag plane. For time $t = 20$ msec, the desired signal component at frequency of 1400 Hz lies within lag $0 < |\tau| < 10$ msec and the interference component at frequency of 1800 Hz lies within lag $10 < |\tau| < 30$ msec. The desired signal component at time $t = 30$ msec with frequency of 1800 Hz occures at lag $0 < |\tau| < 10$ msec and the interference component at frequency of 1400 Hz lies at $10 < |\tau| < 30$ msec.]

4.0 LAG WINDOWED WIGNER-VILLE DISTRIBUTION

The WWVD requires a window that is defined based on some priori information of the signal. As shown in Figure 7, some interference terms were present at the frequency transition regions. A more accurate time-frequency representation is obtained by introducing a time-dependent window in the Wigner-Ville distribution. The resulting time-frequency distribution is known as the lag windowed Wigner-Ville distribution (LWWVD) that is defined as

$$W_{z,lw}(t,f) = \int_{-\infty}^{\infty} h(t,\tau)z(t+\tau/2)z^*(t-\tau/2)\exp(-j2\pi f\tau)d\tau \qquad (5)$$

where $h(t,\tau)$ is the time-dependent window function and is defined over the lag interval $\tau_{win}(t)/2 < \tau < \tau_{win}(t)/2$. Compared to WWVD, the time factor t is included in the definition of the time-dependent window width $\tau_{win}(t)$ to indicate time dependence. The time-dependent window width for $h(t,\tau)$ is calculated for all time instants based on the lag varying characteristics of the bilinear product.

(i) Local lag frequency density (LLFD) method.
(ii) Local lag correlation (LLC) method.

4.1 Local Lag Frequency Density Method

This method uses the variation in the local lag frequency of the bilinear product to estimate the time-dependent window width $\tau_{win}(t)$ for all time instants. Assuming high signal-to-noise ratio conditions, the bilinear product derived from the signal model in Equation (1) is

$$K_z(t,\tau) = K_a(t,\tau)\exp(j\theta(t,\tau)) \tag{6}$$

where $K_a(t,\tau)$ is the envelope and $\theta(t,\tau)$ is the phase of the bilinear product. The local lag frequency density is

$$f_i(t\tau) = \frac{1}{2\pi}\frac{d}{d\tau}(\arg[K_z(t,\tau)]) \tag{7}$$

The local lag frequency density describes the variation in frequency of the bilinear product along the lag axis at a given time instant.

Before the local lag frequency is estimated, it is necessary to determine whether the duration of the signal has zero or low energy. If not, the local lag frequency estimated at this instant will correspond to that of random noise and not of the signal. The instantaneous energy is utilized and evaluated from the bilinear product $K_z(t,0)$. A threshold $E_{z,thd}$ is introduced and is defined as

$$E_{z,thd} = E_{z,\%}\, E_{z,\max}/100 \tag{8}$$

where $E_{z,\%}$ is the user defined threshold value in percentage and $E_{z,\max}$ is the maximum value of $K_z(t,0)$. To include as much details possible about the signal, the user defined threshold value must be set low at the range of $0 < E_{z,\%} < 0.5$.

The local lag frequency is the frequency at a given instant along the lag axis and is defined as

$$f_{i,loc}(t,\lambda) = \int_{-T/2}^{T/2} w(\tau) f_i(t,\tau-\lambda)\,d\tau \tag{9}$$

where T is the analysis frame, $w(\tau)$ is the analysis window function and λ is the instant in lag. The analysis window is

$$w(\tau) = \frac{1}{\tau_w} \qquad \tau_w \to 0, \tau_w \ll \tau_b(t) \tag{10}$$

where τ_w is the analysis window width which is fixed and independent of time and $\tau_b(t)$ is the lag boundary that separates the desired and interference signal

components in lag. If λ is zero, the local lag frequency corresponds to the desired frequency of the signal and the lag boundary $\tau_b(t)$ must lie at $\lambda > 0$ and $\lambda < \infty$ along the lag axis. For a given time instant, the lag boundary is estimated by evaluating the inequality

$$f_{i,loc}(t,0) \neq f_{i,loc}(t,\lambda) \pm f_{i,limit},\ \lambda \in \tau,\ 0 < \lambda < T \tag{11}$$

where, f_{limit} is the acceptable frequency variation in $f_{i,loc}(t,0)$. As λ is varied over the lag axis, the value of l that satisfies the inequality is the estimate of the lag boundary that is used as the time-dependent window width $\tau_{win}(t)$.

To apply the LLFD method, the LWWVD must be set to produce minimum interference in the time-frequency representation. For the signals used for analysis, the user defined threshold value $E_{z,\%}$ used is 0.25, and the acceptable frequency variation f_{limit} is 100 Hz. The difference in the subcarrier frequencies can be as a guide to derive the acceptable frequency variation. If signal FSK0 is used as an example, the subcarrier frequencies are 1400 and 1800 Hz, and the difference in the frequencies or the deviation frequency is 400 Hz. In the bilinear of the signal shown in Figure 6, the frequency difference between the desired and interference signal components is 400 Hz that is equal to the deviation frequency. To determine the location of the lag boundary at a given time instant, it is important to detect the difference in frequency between the desired and interference signal components. Also, there will be some random fluctuations in the subcarrier frequency due to interference such as noise. The choice of the acceptable frequency variation must be greater than the random fluctuations due noise and simultaneously less than the deviation frequency. Experimentally, an acceptable frequency variation of 100 Hz is suitable for signal FSK0. It is found that the same value is also applicable for the rest of the signals defined in Table 1. This is because the acceptable frequency variation depends on the deviation frequency and not the exact value of the subcarrier frequencies.

4.2 Local Lag Correlation Method

The local lag correlation function uses a special form of the correlation function to analyze the lag varying characteristics of the signal and estimate the lag window width for all time instants. By using the definition of the bilinear product in Equation (2), the local lag correlation function is

$$R_{k_z}(t,\lambda) = \int_{-T/2}^{\tau T/2} |w(\tau)|^2\ K_z(t,\tau)\ K_z(t,\tau-\lambda)d\tau \tag{12}$$

where T is the analysis frame, $w(t)$ is the analysis window function and λ is the instant of interest in lag. The window function is a real positive function defined in Equation (10). The local lag correlation function measures the similarity of the bilinear product at $\tau=0$ and at $\tau=\lambda$ averaged within the analysis window τ_w. If the bilinear product at $\tau=0$ and at $\tau=\lambda$ are not equal, the correlation function will be zero. Thus, the amplitude of the local lag correlation function can be used to indicate any miscorrelation of the signal in lag and can be used to estimate the time-dependent window width $\tau_{win}(t)$.

The local lag correlation function is dependent on the amplitude since the computation is based on the average of the product of two signals. To minimize amplitude dependence, the normalized local lag correlation function is used instead and is defined as

$$R_{K_z}(t,\lambda) = \frac{\int_{-T/2}^{T/2} w(\tau)^2 K_z(t,\tau) K_z^*(t,\tau-\lambda)\, d\tau}{\sqrt{E_{K_z}(t,0) E_{K_z}(t,\lambda)}} \tag{13}$$

where

$$E_{K_z}(t,\lambda) = \int_{-T/2}^{T/2} [w(\tau) K_z(t,\tau-\lambda)]^2\, d\tau \tag{14}$$

The possible range of values for the normalized local lag correlation function is

$$0 < |R_{K_z}(t,\lambda)| < 1 \tag{15}$$

The correlation is highest when $[R_{K_z}(t,\tau)]$ has a value of 1.

Since the desired signal component lies close to lag $\tau=0$ in the time-lag plane, the correlation function $[R_{K_z}(t,0)]$ is defined as the reference local lag correlation function and should approach unity. The lag window width $\tau_{win}(t)$ is determined by varying λ such that the following inequality is satisfied

$$|R_{K_z}(t,\lambda)| < R_{K,thd}\ |R_{K_z}(t,0)| \tag{16}$$

where $R_{K,thd}$ is the correlation threshold level. The threshold level is used to decide if the local lag correlation function at a given lag instant λ corresponds to the lag boundary that separates the desired and interference signal components. If satisfied, then the instant λ is the time-dependent window width $\tau_{win}(t)$. Based on the example of the bilinear product in Figure 6, the normalized local lag correlation function evaluated at time instants of 20 and 30 msecs with analysis window width of 5 msec is

$$\begin{aligned} |R_{K_z}(t,\lambda)| &= 1 && \lambda = 0, \lambda \in \tau \\ |R_{K_z}(t,\lambda)| &= 0.1892, && \tau_b(t) < \lambda < 3\tau_b(t) = 0, \lambda \in \tau \\ |R_{K_z}(t,\lambda)| &= 0.45, && \lambda = \tau_b(t), \lambda \in \tau \end{aligned} \tag{17}$$

Similarly if an analysis window width of 6 msec is used, the normalized local lag correlation function evaluated at time instants of 20 and 30 msecs is

$$\begin{aligned} |R_{K_z}(t,\lambda)| &= 1 && \lambda = 0, \lambda \in \tau \\ |R_{K_z}(t,\lambda)| &= 0, && \tau_b(t) < \lambda < 3\tau_b(t) = 0, \lambda \in \tau \\ |R_{K_z}(t,\lambda)| &= 0.5, && \lambda = \tau_b(t), \lambda \in \tau \end{aligned} \tag{18}$$

The normalized local lag correlation function can be used to estimate the position of the lag boundary. From the results in Equation (17) and (18), the range of values for the normalized local lag correlation function at the lag boundary is 0.45-0.5. This range of values is used as the correlation threshold level $R_{K,thd}$ in Equation (16) and a value 0.5 is sufficient to indicate position of the lag boundary.

The LWWVD is used with the local lag correlation function to minimized interference in the time-frequency representation. Before the local lag correlation method is used, it is necessary to check the signal energy level using the procedure described in Section 4.2. For the signals used for analysis, the user defined threshold value $E_{z,\%}$ used is 0.25, the analysis window width τ_w is 5 msecs and the correlation threshold level $R_{K,thd}$ is 0.5.

5.0 RESULTS

The time-frequency representations for signal FSK0 using WWVD and LWWVD for signal-to-noise ratio (SNR) greater than 25 dB are shown in Figure 7 to 9. Comparisons in the time-frequency representations for signals

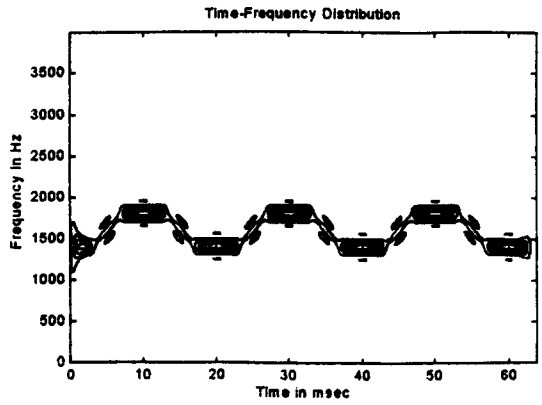

Figure 7 WWVD for signal FSK0 with window width of 5 msec at SNR > 25dB. [Some interference terms are observed at the frequency transition regions.]

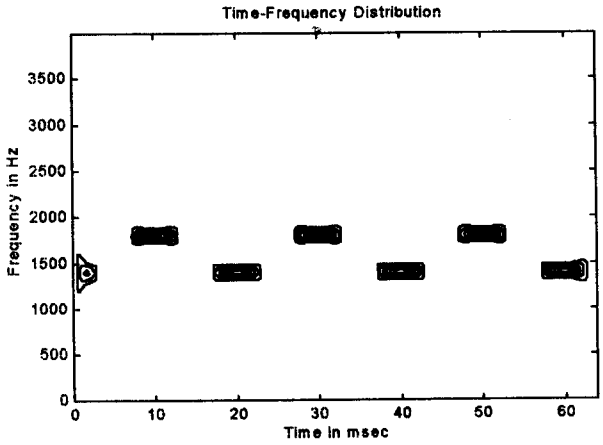

Figure 8 LWWVD with the LLFD method, $E_{z\%} = 0.25, f_{limit} = 100$ Hz at SNR > 25dB. [The time frequency representation is similar to Figure 7 except that no interference terms are observed in the frequency transition regions]

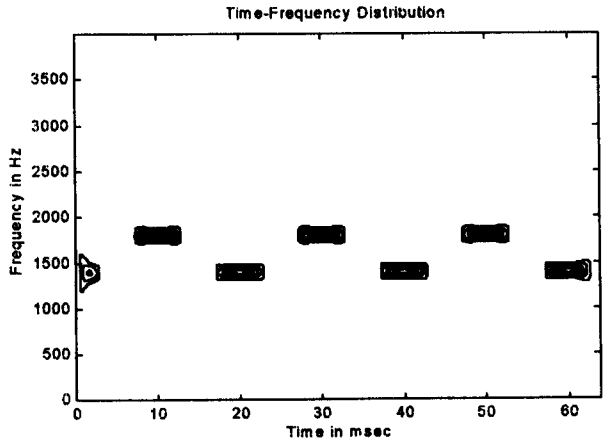

Figure 9 LWWVD with the LLC method, $E_{z\%} = 0.25$, $\tau_w = 5$ msec, $R_{K,thd} = 0.5$ at SNR > 25dB. [Time frequency representation is similar to Figure 8.]

FSK0, FSK0a, FSK1, ASK0 and ASK0a obtained using the RID with exponential kernel, spectrogram, WWVD and the two LWWVD algorithms are presented in Table 2 and Table 3. The criteria for comparisons are made

Table 2 Comparison of the mainlobe width for the time-frequency representations at SNR > 25dB. [A-Spectrogram window width 16 msecs, B-RID with exponential kernel (sigma = 1), C-WWVD window width 5 msec, D-LWWVD local lag frequency density method, $E_{z,\%} = 0.25$, $f_{limit} = 100$ Hz, E-LWWVD local lag correlation function method, $E_{z,\%} = 0.25$, $\tau_w = 5$ msecs, $R_{K,thd} = 0.5$.]

Signal	Mainlobe width (Hz)				
	A	*B*	*C*	*D*	*E*
FSK0	750	205.1	140.9	132.8	140.6
FSK0a	750	54.7	125	46.9	54.7
FSK1	750	187.5	140.6	131.6	140.6
ASK0	750	187.5	140.6	187.6	171.9
ASK0a	750	46.9	125	46.9	46.8
ASK2	200	200.1	140.6	208	174

Table 3 Comparison of the peak-to-sidelobe ratio for the time-frequency representations at SNR > 25dB. [A-Spectrogram window width 16 msecs, B-RID with exponential kernel (sigma = 1), C-WWVD window width 5 msec, D-LWWVD local lag frequency density method, $E_{z,\%} = 0.25$, $f_{limit} = 100$ Hz, E-LWWVD local lag correlation function method, $E_{z,\%} = 0.25$, $\tau_w = 5$ msecs, $R_{K,thd} = 0.5$.]

Signal	Peak-to-sidelobe ratio				
	A	*B*	*C*	*D*	*E*
FSK0	401	29.8	49.9	97.8	52.7
FSK0a	392	50.54	28.9	66.3	61.2
FSK1	573	32.3	49.8	98.5	52.7
ASK0	1200	34.4	48.9	30.9	35.5
ASK0a	1800	50.6	28.9	69.03	61.3
ASK2	617	43.5	52.2	35.5	35.5

based on the mainlobe width and the peak-to-sidelobe ratio. Ideally, the desired mainlobe width should be as narrow as possible and the peak-to-sidelobe ratio should be large. In general, the LWWVD gave the most accurate time-representations for all the signals and this is reflected by the lower mainlobe width and higher peak-to-sidelobe ratio compared to the other methods.

At SNR of 12 dB, the time-frequency representations for signal FSK0 using the WWVD and LWWVD are shown in Figure 10 to 12. A lower SNR

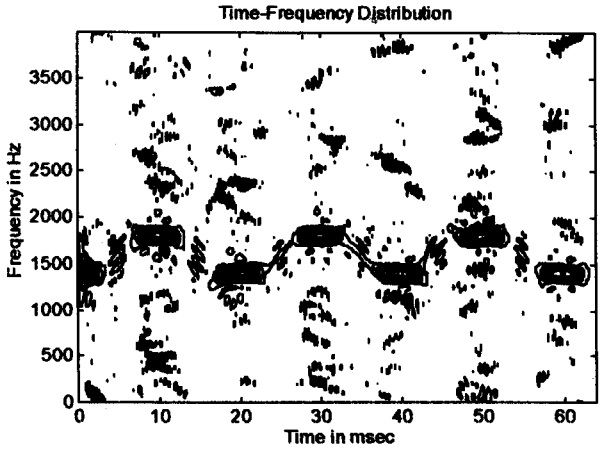

Figure 10 WWVD for signal FSK0 with window width of 5 msec at SNR = 12dB. [Some interference terms over the time-frequency plane due to noise.]

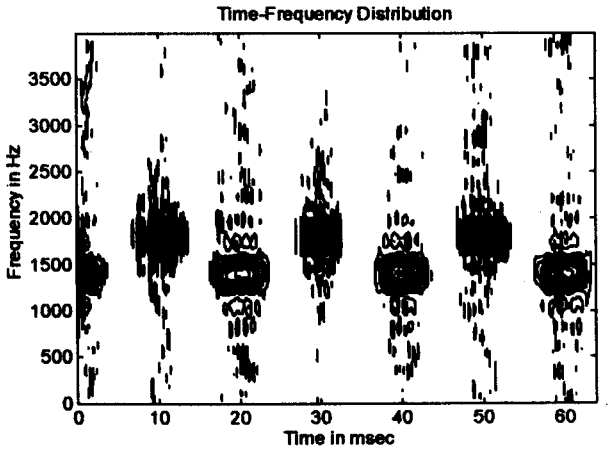

Figure 11 LWWVD with LLFD method, $E_{z,\%} = 0.25, f_{limit} = 100\text{Hz}$ at SNR = 12dB. [The presence of noise causes variation in the time-depent window width resulting in smearing in the time-frequency plane.]

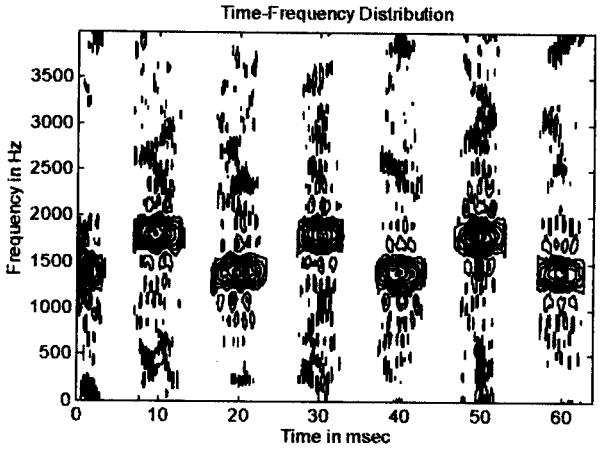

Figure 12 LWWVD with the LLC method, $E_{z,\%} = 0.25$, $\tau_w = 5$ msecs, $R_{K,thd}+0.5$ at SNR > 25dB. [The effect of smearing is less compared to Figure 11.]

indicates a more significant presence of noise in the signal. The effect of noise on the time-frequency representations for signals FSK0, FSK0a, FSK1, ASK0 and ASK0a obtained using the RID with exponential kernel, spectrogram, WWVD and the two LWWVD algorithms are presented in Table 4 and Table 5. Compared to high SNR conditions, there is an increase in the mainlobe width and a reduction in the peak-to-sidelobe ratio for the time-frequency representation using the LWWVD. The LWWVD with the LLC method produce a more accurate time-frequency representation compared to

Table 4 Comparison of the mainlobe width for the time-frequency representations at SNR = 12dB. [A-Spectrogram window width 16 msecs, B-RID with exponential kernel (sigma = 1), C-WWVD window width 5 msec, D-LWWVD local lag frequency density method, $E_{z,\%} = 0.25$, $f_{limit} = 100$ Hz, E-LWWVD local lag correlation function method, $E_{z,\%} = 0.25$, $\tau_w = 5$ msecs, $R_{K,thd} = 0.5$.]

Signal	Mainlobe width (Hz)				
	A	*B*	*C*	*D*	*E*
FSK0	750	201.3	139.9	560	267
FSK0a	750	68.1	130.9	321.1	56.5
FSK1	750	201.3	144.7	440	226.9
ASK0	750	209.4	143.2	453.9	353.9
ASK0a	750	54.68	129.5	292.1	62.5

Table 5 Comparison of the peak-to-sidelobe ratio for the time-frequency representations at SNR = 12dB. [A-Spectrogram window width 16 msecs, B-RID with exponential kernel (sigma = 1), C-WWVD window width 5 msec, D-LWWVD local lag frequency density method , $E_{z,\%} = 0.25$, $f_{limit} = 100$ Hz, E-LWWVD local lag correlation function method, $E_{z,\%} = 0.25$, $\tau_w = 5$ msecs, $R_{K,thd} = 0.5$.]

Signal	Peak-to-sidelobe ratio				
	A	*B*	*C*	*D*	*E*
FSK0	401	33.4	15.6	7	10.6
FSK0a	392	51.9	15.9	11.1	28.5
FSK1	573	32.6	17.1	8.84	12.8
ASK0	1200	35	17.1	8.95	8.95
ASK0a	1800	53.5	16.7	12.4	26.7

the LWWVD with the LLFD method. The degradation in the performance of the LWWVD can be attributed to the variability to estimate the time-dependent width in the presence of noise. This problem is less significant for the spectro-gram, RID and the WWVD since the window width in both the spectrogram and WWVD and the kernel function in the RID are fixed and independent of the characteristics of the signal. In general, the time-frequency representation at lower SNR conditions is more accurate using the RID and WWVD compared to the LWWVD.

The time-frequency representations for real HF data communication signals are shown in Figure 13 to 15 for signal FSK2 and Figure 16 to 18 for signal

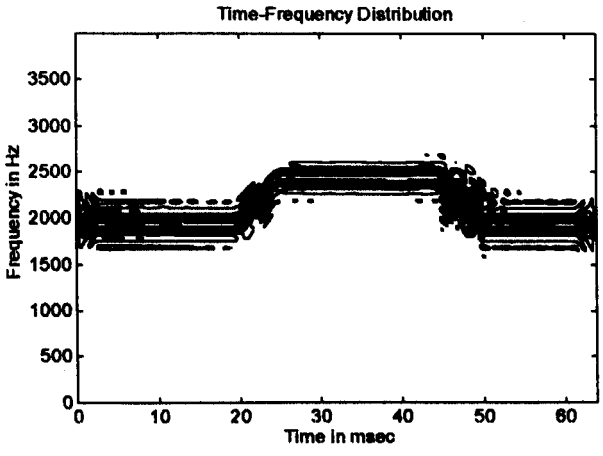

Figure 13 WWVD for real HF data communication signal FSK2 with window width of 5 msec. [Interference terms are observed at the frequency transition regions.]

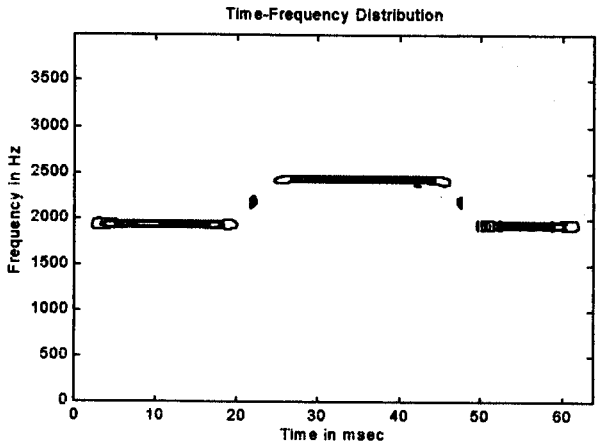

Figure 14 LWWVD with LLFD method, $E_{z,\%} = 0.25$, $f_{limit} = 100$ Hz for real HF data communication signal FSK2. [The time-frequency representation is similar to Figure 13 except the interference terms are observed in the frequency transition regions is minimized.]

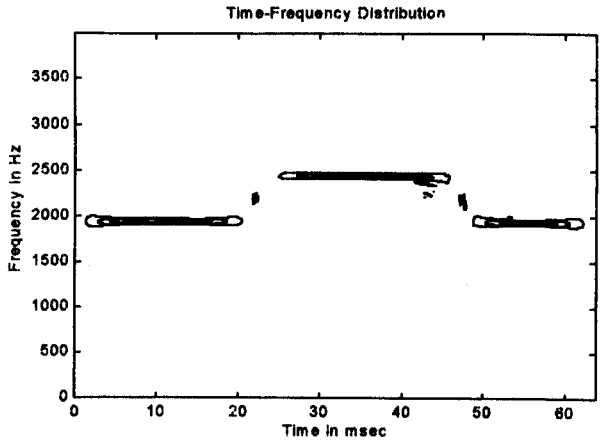

Figure 15 LWWVD with the LLC function method, $E_{z,\%} = 0.25$, $\tau_w = 4$ msecs, $R_{K,thd} = 0.5$ for real HF data communication FSK2 signal. [Time-frequency representation is similar to Figure 14. The effect of noise is mimimal since the signal was measured at high SNR condition.]

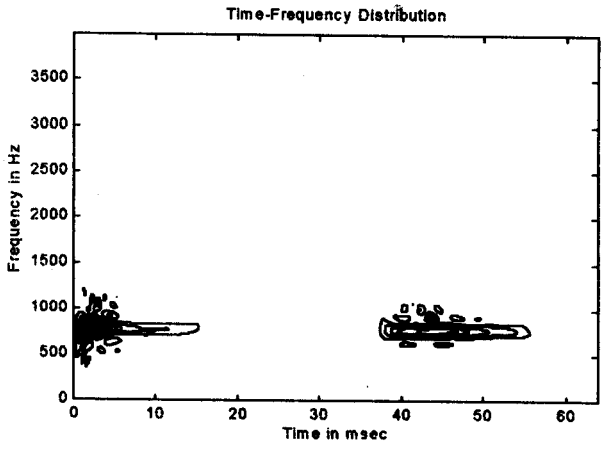

Figure 16 WWVD for real HF data communication signal ASK2 with window width of 5 msec.

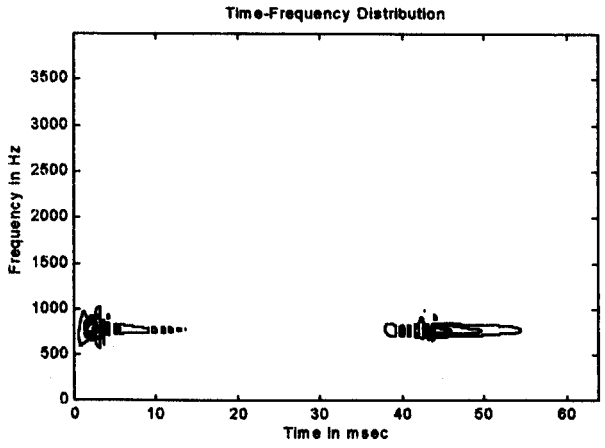

Figure 17 LWWVD with the LLFD method, $E_{z,\%} = 0.25, f_{limit} = 100$ Hz for real HF data communication signal ASK2.

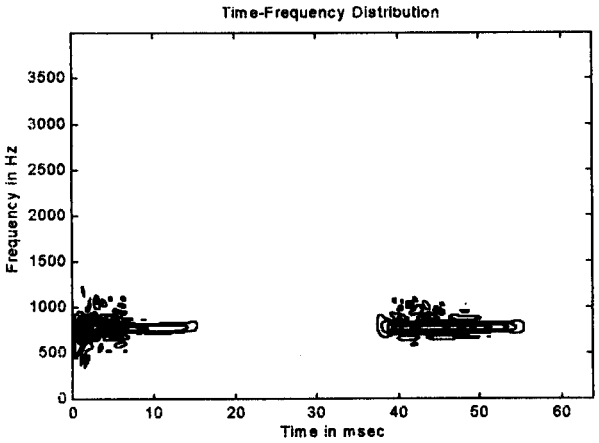

Figure 18 LWWVD with the LLC method, $E_{z,\%} = 0.25$, $\tau_w = 4$ msecs, $R_{K,thd} = 0.5$ for real HF data communication signal ASK2. [Time-frequency representation is similar to Figure 17.]

ASK2. Similar to the simulated signals, the most accurate time-frequency representations for FSK2 can be obtained using the LWWVD. This is shown in Table 2 and 3 where the criteria for comparisons are the mainlobe width and the peak-to-sidelobe ratio. However, this is not true for signal ASK2 where there is no significant improvement in the accuracy of the time-frequency representation. The results in Table 4 and 5 shows that the time-frequency representations degraded if noise is significant at SNR of 12dB. Since ASK2 was measured in the presence of noise, the time-frequency representation based on the WWVD is more accurate in this instant compared to the LWWVD. Therefore, the LWWVD can be used to obtain accurate time-frequency representations for real HF data communication signals at high SNR conditions.

6.0 CONCLUSIONS

The WWVD can be used to provide accurate time-frequency representations for digital modulated signals such as ASK and FSK. Using the LWWVD makes further improvements in the time-frequency representations. The LWWVD is similar to the WWVD except that a time-dependent window in included as part of the algorithm. The time-dependent window width is determined for all time instants according to the characteristics of the signal in time-lag plane. Two methods proposed for estimating the time-dependent window width are the local lag frequency density method and the local lag correlation method. Comparisons with existing time-frequency distributions

such as the spectrogram and the RID with exponential kernel show that the LWWVD gave the most accurate time-frequency representations for the ASK and FSK signals at high SNR conditions. The comparisons are made based on the mainlobe width and the peak-to-sidelobe ratio. For low signal-to-noise ratio, the LWWVD with the LLC method could still produce accurate time-frequency representation compared to the LWWVD with the LLFD method. The results also confirmed that the LWWVD can be used to obtained accurate time-frequency representations for real HF data communications signals.

REFERENCES

[1] "Automatic Monitoring of Occupancy of the Radio Frequency Spectrum", SM.182-4, *ITU-R Recommendations 1997*, SM-Series, Part I.

[2] "Classification and Designation of Emission", Rec 507, *Spectrum Utilization and Monitoring*, Rec and Reports of the CCIR, 1978, XIV th Plenary Assembly, Kyoto, 1978, Vol I, 237-243.

[3] Schreyoegg C., J. Reichert. 1997. Modulation Classification of QAM Schemes Using the DFT of the Phase Histogram Combined with the Modulus Information, *Proc. of 1997 MILCOM Conference*, Part 3 Nov 3-5, Monterey, USA, 1372-76.

[4] Beidas, B.F, C.L Weber. 1998. Asynchronous Classification of MFSK Signals Using the Higher Order Correlation Domain. *IEEE Transactions on Comm.* 46(4):480-493.

[5] Vergara Dominguez L., J.M Paez Borrallo, J. Portillo Garcia and B. Ruiz Mezcua. 1991. A General Approach to the Automatic Classification of Radiocommunication Signals. *Signal Processing*. 22:239-50.

[6] Hsue S.Z and S.S Soliman. 1990. Automatic Modulation Classification Using Zero Crossings. *IEE Proceedings*. 137(6):459-464.

[7] Gardner W.A and C.M Spooner. 1992. Signal Interception:Performance Advantages of Cyclic Feature Detectors. *IEEE Trans on Communications*. 40(1):149-159.

[8] Assaleh K., K. Farrell and R.J Mammone. 1992. A New Method of Modulation Classification for Digitally Modulated Signals. *Proceedings of MILCOM 92*. San Diego: 11-14 Oct 1992, 712-16.

[9] Claasen T. and W. Macklenbrauker. 1980. The Wigner Distribution-The Tool for Time-Frequency Signal Analysis: Part I; Continuous-Time Signal. *Phillips Journal of Research*. 35:217-250.

[10] Boashash B. 1990. Time-Frequency Signal Analysis. In S. Haykin (ed.) *Advances in Spectrum Estimation and Array Processing* Vol. 1, Prentice-Hall, 418-517.

[11] Jeong J. and W.J Williams. 1989. Kernel Design for Reduced Interference Distributions. *IEEE Trans. Signal Processing*. 40(2):402-412.

[12] Boashash B., and P. O'Shea. 1994. Polynomial Wigner-Ville Distribution and Their Relationship to Time-Varying Higher-Order Sprectra. *IEEE Trans. Signal Processing*. 42(1):216-220.

[13] Emresoy M.K. and A. El-Jaroudi. 1988. Iterative Instantaneous Frequency Estimation and Adaptive Matched Spectrogram. *Signal Processing*. 64(2):157-165.

[14] Andria G., M. Savino. 1996. Interpolated Smooth Pseudo Wigner-Ville distribution for Accurate Spectrum Analysis. *IEEE Trans. on Instrumentation and Measurement*. 45(4):818-823.

[15] Wang C. and M.G Amin. 1998. Interference Mitigation in Spread Spectrum Communication Systems Using Time-Frequency Distributions. *IEEE Trans. Signal Processing*. 46(1):90-101.

[16] Pei S.C and T.Y Wang. 1987. *Modulation Signal Classification by Wigner Distribution*. ISSPA87, Brisbane, Australia, 24-28, 269-274.

[17] Roessgen M. and B. Boashash. 1994. Time-Frequency Peak Filtering Applied to FSK Signals. *IEEE-SP Int. Symp. on Time-Freq & Time-Scale Analysis*. USA: Philadelphia, 25-28, 516-519.

[18] Boashash B. 1992. Estimating & Interpreting the Instantaneous Frequency of a Signal-Part I: Fundamentals. *Proc. of the IEEE*. 80(4):519-538.